Optical losses characterization in waveguides through the photodeflection method

Mario Bertolotti, MEMBER SPIE
Università di Roma ''La Sapienza''
Dipartimento di Energetica
Istituto Nazionale di Fisica della Materia
Gruppo Nazionale di Elettronica Quantistica e Plasmi
Via Scarpa 16
00161 Roma, Italy
E-mail: bertolotti@axrma.uniroma1.it

G. Liakhou
Technical University of Moldova
Shtephan Cel Mare
277012 Kishinev, Moldova

R. Li Voti
A. Matera
Concita Sibilia
M. Valentino
Università di Roma ''La Sapienza''
Dipartimento di Energetica
Istituto Nazionale di Fisica della Materia
Gruppo Nazionale di Elettronica Quantistica e Plasmi
Via Scarpa 16
00161 Roma, Italy

Abstract. The photodeflection method is able to characterize the propagation losses in optical waveguides. The theory of the transverse configurations in air and *in situ* is reviewed. The procedure to determine the propagation loss coefficient is widely discussed. The experimental results on two different Ti:$LiNbO_3$ and glass channel waveguides are in good agreement with theory.

Subject terms: photoacoustic and photothermal science and engineering; photodeflection method; optical waveguides; propagation losses.

Paper PPS-03 received June 14, 1996; accepted for publication Aug. 20, 1996.

1 Introduction

Optical waveguides are the basic components for the fabrication of most integrated optical devices such as modulators, filters, and sensors. The determination of the attenuation coefficient of the optical power traveling in the guide, which depends on the propagation losses (i.e., absorption, scattering) is one of the most important characterizations. A number of different methods have been developed in the past. The main idea, common to several techniques, is to calculate the propagation losses starting from the decay, in the direction of propagation, of any signal (thermal, optical, electrical) proportional to the guided light intensity (sliding prism,[1] pyroelectric,[2] and out-of-plane scattered light[3] methods). Other techniques enable one to estimate losses by measuring the quantity of heat generated in the sample (calorimetric[4] method) or by measuring the width of the fringes of the optical resonator[5–7] obtained by polishing the waveguide endfaces. Recently a new method based on the photodeflection (PD) effect has been proposed and used.[8] In general the PD technique analyzes the deflection of a test laser beam (probe) traveling in a medium with a thermally induced refractive index gradient[9,10,11] from its originary trajectory. For both planar and channel waveguides, the refractive index gradient is due to the thermal gradient produced when the guided light, which is a prism or an end-fire-coupled time-modulated pump laser beam, is absorbed during the propagation. Compared with the previous techniques, PD presents several advantages, including being nondestructive, contactless, independent on the optical coupling system, and applicable to a wide range of both planar and channel waveguides with different geometry (buried channel, raised or embedded strip, rib or ridge guide) and materials.[11,12] In the following, the determination of the temperature rise and of the PD angle are discussed for a waveguide system, and some experimental results are given.

2 Theory

To investigate the optical properties of a waveguide, generally a pump light beam is coupled at the input edge of the waveguide (end-fire, prism coupling) and is kept under observation during the propagation through the allowed modes. In most cases, the beam intensity is uniformly attenuated along the guide due to different loss processes (absorption, scattering), giving rise to an exponential decay profile. The absorption processes produce a temperature rise T along the waveguide and in the surrounding medium (air), which can be measured to reconstruct the intensity profile. Note that all the photothermal techniques that enable contactless measurement of temperature rise profile (i.e., radiometry) or the thermal gradient profile (i.e., PD) use a periodical regime of heating to reduce the experimental noise. According to this requirement, before coupling in the guide, the pump beam is intensity modulated by means of a mechanical chopper working in the range of audio frequencies (1 Hz to 4 kHz).

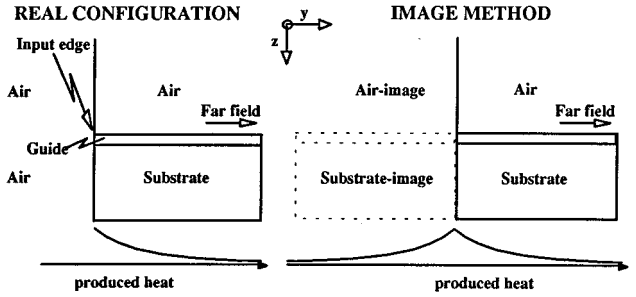

Fig. 1 Configuration.

In the following, we give the solution of the Fourier heat equation in the harmonic regime and discuss the temperature rise for different kinds of waveguides (planar and channel). In any case, the starting equation is the differential equation for heat conduction, which is written in the harmonic regime as

$$\nabla^2 T_i - \frac{j\omega}{D_i} T_i = -\frac{w}{k}, \tag{1}$$

where T, D, and k are the temperature rise, the thermal diffusivity, and the thermal conductivity for each thermally distinguished medium; ω is the angular frequency of the periodical heating process, w is the optical power density transformed into heat (heat power density), which, by assuming the guide to be single mode and the loss processes to be uniform, can be written as

$$w = \alpha_{\text{th}} I_0(x,z) e^{-\alpha y} \quad y>0, \tag{2}$$

where I_0 is the intensity of the guided mode at the input edge ($y=0$), α is the total losses coefficient of the mode, and α_{th} is the fraction of α due to absorption only. In case of a multimode guide, the expression for w is given by the superposition of the w's related to each mode. Particular care must be paid to the boundary conditions of Eq. (1), which imply the continuity of the temperature rise T at each interface S between two different media and the conservation of the thermal flux $k(\mathrm{d}T/\mathrm{d}n)$ crossing S. The exact solution for T cannot be given in a closed form due to the complexity of the boundaries (see Fig. 1) and numerical methods (FDM) or a Schwarz-Christoffel transformation must be used to solve it. Other methods based on the bad thermal conductivity of the air provide a handy and accurate approximation that tends to the exact one far from the input edge (far thermal field). They basically consist of neglecting the heat losses from the input edge of the guide toward the air. This enables one to consider the half-space $y<0$ as a vacuum and to apply the image method for the other half-space $y>0$ (see Fig. 1). The main result is that the solution for T is given by a simpler geometrical system made of air ($z<0$) and the substrate-waveguide system ($z>0$), where the edge in $y=0$ is removed; the resulting structure is heated by both the heat power density given by Eq. (2) and its image for $y<0$. In many cases, the guiding layer is obtained by doping the substrate to enhance its refractive index, which is usually about 1 μm thick so that we can assume the substrate-waveguide system, from the thermal point of view, is a single medium. Therefore, Eq. (1) together with the boundary conditions can be rewritten as

$$\begin{cases} \nabla^2 T_{\text{air}} - j\omega/D_{\text{air}} T_{\text{air}} = 0 & z<0 \\ \nabla^2 T_{\text{sub}} - \dfrac{j\omega T_{\text{sub}}}{D_{\text{sub}}} \\ \qquad = -\dfrac{\alpha_{\text{th}} I_0(x,z)\ \exp\ (-\alpha|y|)}{k_{\text{sub}}} & z>0 \\ k_{\text{air}} \left.\dfrac{\mathrm{d}T_{\text{air}}}{\mathrm{d}z}\right|_{z=0} = k_{\text{sub}} \left.\dfrac{\mathrm{d}T_{\text{sub}}}{\mathrm{d}z}\right|_{z=0} \\ T_{\text{air}}|_{x=0} = T_{\text{sub}}|_{z=0}, \end{cases} \tag{3}$$

where the subscript sub stands for the substrate. The details of the solution of Eq. (3) are given in Appendix A. The temperature rise in air far from the edge (far thermal field) is given for a channel waveguide by

$$T(x,y,z) = \frac{1}{2\pi^2} \int \int_{-\infty}^{+\infty} \frac{\alpha \alpha_{\text{th}} P}{(k_{\text{sub}}\beta_{\text{sub}} + k_{\text{air}}\beta_{\text{air}})(\alpha^2 + \delta_y^2)} \times \exp\ (-\beta_{\text{air}} z)\ \exp\ [i(\delta_x x + \delta_y y)]\ \mathrm{d}\delta_x\ \mathrm{d}\delta_y\,; \tag{4}$$

while for a planar waveguide it is

$$T(x,y,z) = \frac{1}{\pi} \int_{-\infty}^{\infty} \frac{\alpha \alpha_{\text{th}} P}{(k_{\text{sub}}\beta_{\text{sub}} + k_{\text{air}}\beta_{\text{air}})(\alpha^2 + \delta_y^2) a} \times \exp\ (-\beta_{\text{air}} z)\ \exp\ [i(\delta_y y)]\ \mathrm{d}\delta_y\,. \tag{5}$$

The integrals in Eqs. (4) and (5) are not given in a closed form, but can be solved with a computer. The main result is that by performing a scan along the direction of propagation (y), both Eqs. (4) and (5) show an exponential behavior in y from which the value of the total losses coefficient α can be determined.

3 PD Technique

Generally, the PD effect consists of the bending of a probe laser beam due to the thermal gradients along the beam path (mirage). This is the basic effect used for the detection of many photothermal phenomena. The theory shows that the deflection from the originary trajectory of the probe beam is in the plane transverse to the beam path and depends on the thermal gradients in the direction orthogonal to the path only, according with the well-known formula (geometric optics)

$$\Phi = \frac{1}{n} \left(\frac{\mathrm{d}n}{\mathrm{d}T} \right) \nabla_t \int_{\text{path}} T(x,y,z)\ \mathrm{d}s, \tag{6}$$

where n and $\mathrm{d}n/\mathrm{d}T$ represent the refractive index and the optothermal parameter of the crossed medium, T is the temperature rise in air, and ∇_t is the gradient transverse to the path s. To characterize the propagation losses, the PD angle must be measured along the guide (y direction). This

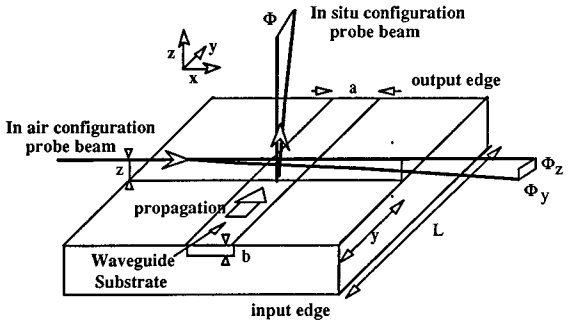

Fig. 2 Experimental setup: configuration in air and *in situ*.

requirement sets the probe beam path to be transverse to the propagation axis and hence to the pump beam. Two different choices for the probe beam path are available: the configuration in air or *in situ* (see Fig. 2). In the configuration in air, the probe skims in the air as close as possible to the guide. Sometimes, if the waveguide is able to reflect the probe, a stronger signal can be obtained by bouncing the probe laser beam near the guide with a small tilt angle and by measuring the deflection angle of the reflected beam. The configuration in air is usually applied when a physically contactless detection system is needed (photorefractive or probe-absorbing waveguides). The deflection angle $\mathbf{\Phi}$ has two components of which the one directed along the z axis Φ_z is larger than the one along the propagation direction Φ_y. By combining Eq. (6) with Eqs. (4) and (5) and by using the properties of the Dirac function, we find that the expressions of the deflection angle in the far field coincide for both planar and channel waveguides and are

$$\begin{cases} \Phi_y = \dfrac{-2}{n}\dfrac{\mathrm{d}n}{\mathrm{d}T}\dfrac{\alpha\alpha_{\mathrm{th}}P}{\pi}\displaystyle\int_0^\infty \dfrac{\delta \sin(\delta y)\,\exp(-\beta_{\mathrm{air}} z)\,\mathrm{d}\delta}{(k_{\mathrm{sub}}\beta_{\mathrm{sub}}+k_{\mathrm{air}}\beta_{\mathrm{air}})(\alpha^2+\delta^2)} \\ \Phi_z = \dfrac{2}{n}\dfrac{\mathrm{d}n}{\mathrm{d}T}\dfrac{\alpha\alpha_{\mathrm{th}}P}{\pi}\displaystyle\int_0^\infty \dfrac{\beta_{\mathrm{air}} \cos(\delta y)\,\exp(-\beta_{\mathrm{air}} z)\,\mathrm{d}\delta}{(k_{\mathrm{sub}}\beta_{\mathrm{sub}}+k_{\mathrm{air}}\beta_{\mathrm{air}})(\alpha^2+\delta^2)}. \end{cases} \tag{7}$$

In general, the integrals in Eqs. (7) must be solved numerically, but an exception exists in the case of an optical penetration $1/\alpha$ larger than the thermal diffusion length of each medium, defined as $\ell = (D/\pi f)^{1/2}$. In this case, which is usually verified also for bad guides ($\alpha = 10\ \mathrm{cm}^{-1}$), Eqs. (7) can be greatly simplified and become

$$\begin{cases} \Phi_y = \dfrac{-1}{n}\dfrac{\mathrm{d}n}{\mathrm{d}T}\dfrac{\alpha_{\mathrm{th}}P}{k_{\mathrm{sub}}}\dfrac{\alpha\ell}{(1+j)}\exp[-\alpha y-(1+j)z/\ell_{\mathrm{air}}] \\ \Phi_z = \dfrac{1}{n}\dfrac{\mathrm{d}n}{\mathrm{d}T}\dfrac{\alpha_{\mathrm{th}}P}{k_{\mathrm{sub}}}\left(\dfrac{D_{\mathrm{sub}}}{D_{\mathrm{air}}}\right)^{1/2}\exp[-\alpha y-(1+j)z/\ell_{\mathrm{air}}], \end{cases} \tag{8}$$

in which the air thermal conductivity term has been neglected. Equations (8) are the proof of our expectations. They show that

1. The lateral component is smaller than the vertical one, being proportional to $\alpha\ell$, which is much smaller than $(D_{\mathrm{sub}}/D_{\mathrm{air}})^{1/2}$.
2. Both components of the deflection angle have an exponential behavior with αy.
3. Both components of the deflection angle depend strongly on the height z of the probe beam from the surface. In particular, the phase and the logarithm of the amplitude of Φ decrease proportionally to the height, normalized to the air thermal diffusion length z/ℓ_{air}.

To determine the total losses, in principle, one must perform a scan in the y direction at a fixed height z. By plotting the amplitude in a log scale, a linear slope is found that directly gives the value of α. But in practice when the scan is performed, a setup misalignment always occurs so that z cannot be considered constant. If we take into account the tilt angle θ between the surface and the scan line, then the height z depends on y as follows $z = y\tan(\theta)$. If we introduce this value for z into Eqs. (8), the attenuation α' calculated with the standard procedure differs from the right value α according to the relationship[12]

$$\alpha' = \alpha + \frac{\tan(\theta)}{(D_{\mathrm{air}})^{1/2}}\sqrt{\pi f}. \tag{9}$$

An elegant way to correct for the misalignment and to obtain the right α is measuring the attenuation for different values of the chopper frequency. In fact, by plotting α' as a function of the frequency square root, a straight line is obtained from which both α and θ are calculated. Another effect of the misalignment is the dependence, absent for z constant, of the phase signal versus y:

$$\varphi = \varphi_0 + \frac{\tan(\theta)}{(D_{\mathrm{air}})^{1/2}}\sqrt{\pi f}y, \quad \frac{\mathrm{d}\varphi}{\mathrm{d}y} = \frac{\tan(\theta)}{(D_{\mathrm{air}})^{1/2}}\sqrt{\pi f}. \tag{10}$$

A comparison of Eqs. (10) and (9) clarifies that the excess of attenuation is present in the same way in the phase signal also. Therefore another way to obtain α is given by analyzing both phase and amplitude and subtracting the quantity $d\varphi/dy$ from α'. With this method, total losses of the order of 1 cm^{-1} have been measured. Note that the method does not provide an acceptable accuracy for very low loss waveguides, when no relevant attenuation is detected along the whole guide and the log plot of amplitude has too weak a slope. In this case, a different method must be used based on the analysis in the near thermal field (first few micrometers from the edge) of the deflection angle in the configuration *in situ*. In that region, we cannot neglect the heat losses at the input edge, which are, by the way, responsible for the basic phenomena of the undeflected beam. The use of the configuration *in situ* (see Fig. 2) for low propagation losses, guarantees a stronger signal because of the high value of the solid's optothermal parameter with respect to that of the air. The probe beam is now focused into the waveguide, crossing the whole sample. In this configuration, the deflection angle has a component only along the channel direction. To provide a quantitative expression for

the deflection angle, the theoretical model for the temperature distribution, which mainly takes into account the input edge losses, gives

$$\Phi \propto \exp(-\alpha y) - \frac{\alpha \ell_{wg} + e(1+i)}{(1+e)\alpha \ell_{wg}} \exp\left(-\frac{1+i}{\ell_{wg}} y\right), \quad (11)$$

where

$$\ell_{air/wg} = \left(\frac{2D_{air/wg}}{\omega}\right)^{1/2},$$

$$e = \frac{e_{air}}{e_{wg}} = \left[\frac{k_{air}(\rho c)_{air}}{k_{wg}(\rho c)_{wg}}\right]^{1/2} = \frac{k_{air}}{k_{wg}}\left(\frac{D_{wg}}{D_{air}}\right)^{1/2} = \frac{k_{air}\ell_{wg}}{k_{wg}\ell_{air}},$$

ρ, and c are the thermal diffusion length, the thermal effusivity ratio, the density, and the heat capacity, respectively. The deflection angle depends on two exponential terms that have different decay lengths connected, respectively, with the thermal diffusion and the optical propagation. The thermal diffusion exponential term has importance only for the first few micrometers ($y \ll \ell_{ch}$), being negligible for longer distances from the input edge (far field). In the analysis for a short distance (near field), the diffusion exponential term cannot be neglected with respect to the absorption term. Considering the phase of the two terms, however, it is possible to find some length y_{min} for which the two exponentials have opposite sign so that a minimum in the deflection signal is obtained corresponding to a maximum in temperature. Using a computer one can find that if this minimum exists inside the waveguide, it is independent from the modulation frequency and depends only on the thermal effusivity ratio e (thermal losses) and the propagation loss coefficient α, giving the empirical relation[11]

$$\alpha y_{min} = \ln(1+e) \approx e \quad \text{from which} \quad \alpha = \frac{e}{y_{min}}, \quad (12)$$

which is useful only if $\alpha \ell_{ch} \gg e$. Note that the low value of e (0.001) is of help both for the existence condition and to establish the position at some distance from the edge.

Finally, note that in all methods, the absolute value of the deflection angle is of no importance; only its relative behavior with respect to the position along the waveguiding direction needs to be determined.

Table 1 Slope, phase derivative, and difference values.

f (Hz)	α' (cm^{-1})	dφ/dy (cm^{-1})	Difference (cm^{-1})
16	21.2±0.14	11.7±0.14	9.5
36	24.7±0.5	15.6±0.5	9.1
64	35 ±1	25.4±1	9.6
121	42.6±1.4	34.2±0.6	8.4
225	54.8±0.9	46.5±0.7	8.3
400	68 ±1	60 ±1	8
900	80 ±3	72 ±3	8

4 Experimental Results

The channel waveguide used to test the first method by measuring the exponential decay of the deflection signal was a glass substrate with six channels each 3 μm wide, obtained by ion exchange. The refractive index of substrate is 1.55 with an increase in each channel of about 0.005. Figure 3 shows the logarithm of amplitude of Φ_y versus y in micrometers for different frequencies. Note that starting from a certain distance, the experimental curves have a linear behavior. The different slopes (α') are reported in Table 1 and plotted in Fig. 4 as a function of frequency square root. As previously discussed, the apparent loss coefficient α' depends linearly on the square root of the frequency (squares in Fig. 4). The value of the tilt angle that produces this effect can easily be calculated to be 15 deg, and when the straight line is extrapolated to zero frequency, the intercept is the real α, which results in ~9 cm^{-1} (±10%). The line with crosses in the figure is the experi-

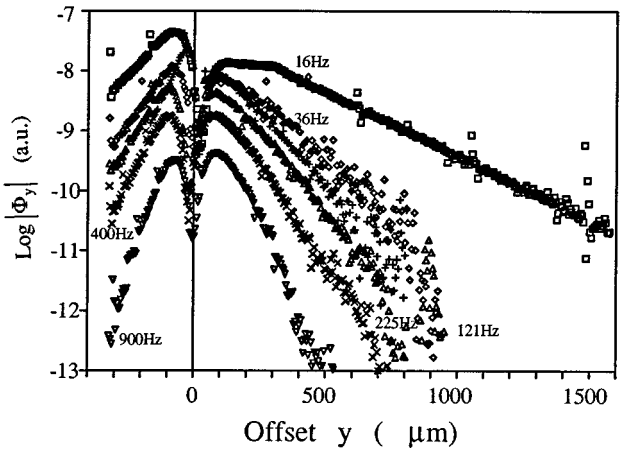

Fig. 3 Experimental results on the glass waveguide: logarithm of the amplitude versus the offset from the edge: the chopper frequencies are f=16, 36, 121, 225, 400, 900 Hz; the measured loss is $\alpha \approx 9$ cm^{-1}.

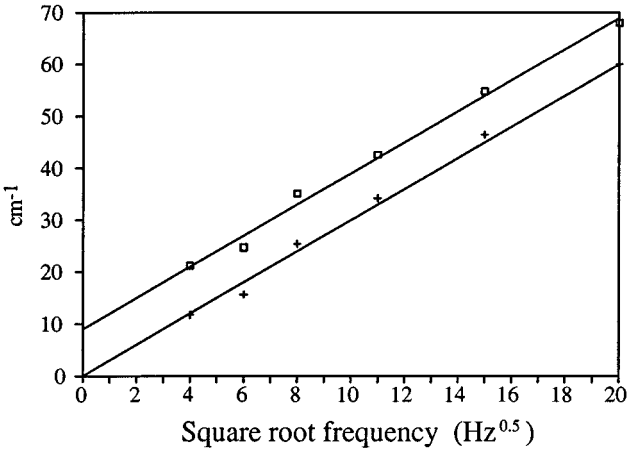

Fig. 4 Squares are the attenuation α', crosses are dΦ/dy in inverse centimeters versus the frequency square root, and the continuous lines are given by the best fit method.

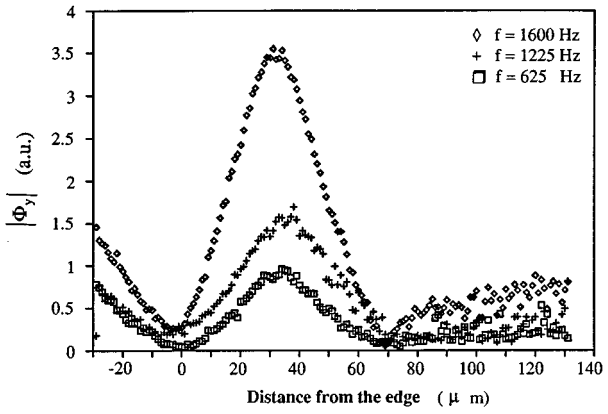

Fig. 5 Experimental results for the Ti:$LiNbO_3$ waveguide: the amplitudes of the deflection angle are for different frequencies as a function of the distance from the edge. The measured loss is $\alpha \approx 0.25$ cm^{-1}: squares, 625 Hz; crosses, 1225 Hz; and diamonds, 1600 Hz.

mental $d\phi/dy$ values. It is exactly parallel to the α' line, as expected from Eqs. (9) and (10) and crosses the origin of the axes.

In columns 3 and 4 of Table 1 the derivative of the phase and the difference with α' are reported. As an example of a waveguide with low losses, the experimental results for a Ti:$LiNbO_3$ channel waveguide are reported. The value of the effusivity ratio at room temperature is about $e \approx 0.0012$. The measurements reported in Fig. 5 are made at different chopper frequencies $f = 625$, 1225, and 1600 Hz. Note that the minimum does not change its position. The estimate of $y_{\min}$ is about 70 μm, which gives rise to a propagation loss coefficient of about $\alpha = 0.17$ cm^{-1} ($\pm 10\%$). The fit is in good agreement with the value given by other techniques.

5 Appendix A

The solution of Eq. (3) depends basically on the intensity profile I_0 of the guided mode; in the following, we deal with two different kinds of waveguides: channel and planar waveguides. For a channel waveguide, the typical small section used for light propagation enables us to assume for the intensity profile the simple expression $I_0(x,z) = P\Delta(x)\Delta(z)$, where Δ is the Dirac function and P is the optical power coupled at the edge. For a planar waveguide, the light is again well localized in z but is spread in a wide region a along the x axis so that $I_0(z) = P\Delta(z)/a$. In any case, the solution of Eq. (3) is given by using the spatial Fourier transform method. The method enables us to define an auxiliary transformed domain of the plane xy (δ_x, δ_y) in which we can study the transformed temperature rise t, which is linked to T by the following direct and inverse formulas:

$$T(x,y,z) = \frac{1}{4\pi^2} \int \int_{-\infty}^{+\infty} t(\delta_x, \delta_y, z) \exp[j(\delta_x x + \delta_y y)] \, d\delta_x \, d\delta_y \Leftrightarrow t(\delta_x, \delta_y, z) = \int \int_{-\infty}^{+\infty} T(x,y,z) \exp[-j(\delta_x x + \delta_y y)] \, dx \, dy. \tag{13}$$

In this domain, Eq. (3) becomes

$$\begin{cases} \dfrac{d^2 t_{\text{air}}}{dz^2} - \beta_{\text{air}}^2 t_{\text{air}} = 0 & z < 0 \\ \dfrac{d^2 t_{\text{sub}}}{dz^2} - \beta_{\text{sub}}^2 t_{\text{sub}} \end{cases} \tag{14}$$

$$= - \int \int_{-\infty}^{+\infty} \frac{\alpha_{\text{th}} I_0(x,z) \exp(-\alpha|y|) \exp[-j(\delta_y y + \delta_x x)]}{k_{\text{sub}}} \times dx \, dy \quad z > 0,$$

where $\beta = (\delta_x^2 + \delta_y^2 + j\omega/D)^{1/2}$. The general solution for t is given by an exponential function in z:

$$\begin{cases} t_{\text{air}} = A^{\beta_{\text{air}} z} & z < 0 \\ t_{\text{sub}} = B^{-\beta_{\text{sub}} z} & z > 0, \end{cases} \tag{15}$$

where the factors A and B are given by the boundary conditions of continuity of temperature and normal heat flux at $z = 0$ according to the relationships

$$\begin{cases} t_{\text{air}}|_{z=0} = t_{\text{sub}}|_{z=0} \Rightarrow A = B \\ \alpha_{\text{th}} \int \int \int I_0(x,z) \exp(-\alpha|y| - j\delta_x x - \delta_y y) \, dx \, dy \, dz \end{cases} \tag{16}$$

$$= -k_{\text{sub}} \frac{dt_{\text{sub}}}{dz} + k_{\text{air}} \frac{dt_{\text{air}}}{dz}$$

$$\Rightarrow \begin{cases} \text{channel} \quad A = \dfrac{2\alpha\alpha_{\text{th}} P}{(k_{\text{sub}}\beta_{\text{sub}} + k_{\text{air}}\beta_{\text{air}})(\alpha^2 + \delta_y^2)} \\ \text{planar} \quad A = \dfrac{\alpha\alpha_{\text{th}} P 2 - \pi\Delta(\delta_x)/a}{(k_{\text{sub}}\beta_{\text{sub}} + k_{\text{air}}\beta_{\text{air}})(\alpha^2 + \delta_y^2)}. \end{cases}$$

The temperature rise in air is given by the Fourier antitransformation of Eq. (3):

$$T(x,y,z) = \frac{1}{4\pi^2} \int \int_{-\infty}^{+\infty} A \exp(-\beta_{\text{air}} z) \times \exp[j(\delta_x x + \delta_y y)] \, d\delta_x \, d\delta_y, \tag{17}$$

which for a channel waveguide gives rise to the expression

$$T(x,y,z)=\frac{1}{2\pi^2}\int\int_{-\infty}^{+\infty}\frac{\alpha\alpha_{\text{th}}P}{(k_{\text{sub}}\beta_{\text{sub}}+k_{\text{air}}\beta_{\text{air}})(\alpha^2+\delta_y^2)}\times\exp(-\beta_{\text{air}}\,z)\,\exp[j(\delta_x x+\delta_y y)]\,\mathrm{d}\delta_x\,\mathrm{d}\delta_y\,, \tag{18}$$

and for a planar waveguide is

$$T(x,y,z)=\frac{1}{\pi}\int_{-\infty}^{\infty}\frac{\alpha\alpha_{\text{th}}P}{(k_{\text{sub}}\beta_{\text{sub}}+k_{\text{air}}\beta_{\text{air}})(\alpha^2+\delta_y^2)a}\times\exp(-\beta_{\text{air}}\,z)\,\exp[j(\delta_y y)]\,\mathrm{d}\delta_y\,. \tag{19}$$

References

1. H. P. Weber, F. A. Dunn, and W. W. Leibolt, ''Loss measurement in thin film optical waveguides,'' *Appl. Opt.* **12**, 755 (1973).
2. A. M. Glass, I. P. Kaminov, A. A. Aliman, and D. H. Olson, ''Absorption loss and photorefractive index changes in Ti:$LiNbO_3$,'' *Appl. Opt.* **19**, 276 (1980).
3. Y. Okamura, S. Yoshinaka, and S. Yamamoto, ''Measuring mode propagation losses of integrated optical waveguide: a simple method,'' *Appl. Opt.* **22**, 3892 (1983).
4. K. H. Heagele and R. Ulrich, ''Pyroelectric loss measurement in $LiNbO_3$:Ti guides,'' *Opt. Lett.* **4**, 60 (1980).
5. I. P. Kaminov and L. W. Stulz, ''Loss in cleaved Ti-diffused $LiNbO_3$ waveguides,'' *Appl. Phys. Lett.* **33**, 62 (1978).
6. R. Reganer and W. Sohler, ''Loss in low-finesse Ti:$LiNbO_3$ optical waveguide resonators,'' *Appl. Phys. B* **36**, 143 ( ).
7. S. V. Bessonova, K. S. Buritskii, V. A. Chenykh, E. A. Shcherbakov, ''Determination of losses in lithium niobate optical waveguides using a single frequency semiconductor laser,'' *Sov. J. Quantum Electron.* **19**, 559 (1989).
8. R. K. Hickeneil, D. R. Larson, R. J. Phelan, and L. Larson, ''Waveguide loss measurement using photothermal deflection,'' *Appl. Opt.* **27**, 1637 (1988).
9. W. B. Jackson, N. M. Amer, D. Fournier, and A. C. Boccara, ''Photothermal deflection spectroscopy and detection,'' *Appl. Opt.* **20**, 1333 (1981).
10. M. Bertolotti, L. Fabbri, E. Fazio, R. Li Voti, C. Sibilia, G. Leakhou, and A. Ferrari, ''Influence of probe absorption in photothermal deflection technique,'' *J. Appl. Phys.* **69**, 3421 (1991).
11. R. Li Voti, M. Bertolotti, G. Liakhou, A. Matera, C. Sibilia, and M. Valentino, ''Optical losses characterization of channel waveguides through a photodeflection method,'' Chap. 18 in *Advances in Integrated Optics*, S. Martellucci, Ed., pp. 273–277, Plenum Press, New York (1994).
12. M. Bertolotti, G. Liakhou, R. Li Voti, A. Matera, C. Sibilia, and M. Valentino, ''Optical losses characterization in channel waveguide through the photodeflection method,'' *J. Physique IV* **C7**, 647 (1994).

Mario Bertolotti received his laurea degree in physics in 1957. He is a full professor of physics in the Universita' di Roma La Sapienza. He is the author of more than 300 papers in the field of quantum electronics and nonlinear optics, as well as several books on quantum electronics.

G. Liakhou received his MS in electronic engineering in 1974 in the USSR. He received his Doctor of Sciences degree in semiconductor physics in the USSR in 1982 and his PhD degree in electromagnetism in Italy in 1995. He works in the field of quantum electronics in Kishinev, Moldova, in the radio electronic faculty of the Technical University of Moldova.

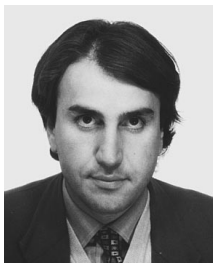

R. Li Voti received his MS degree, magna cum laude, in electronic engineering in 1992. He received the degree of specialist in telecommunication in 1994. He received his PhD degree in electromagnetism in Italy in 1996. He works in the field of quantum electronics in Roma, Italy, in the Dipartimento di Energetica.

A. Matera received his MS degree in electronic engineering in 1993. He received the degree of specialist in telecommunication in 1994.

Concita Sibilia received her laurea degree in physics. She is an associate professor of physics in the Universita' di Roma La Sapienza. She works in the field of quantum electronics and is the author of more than 150 papers.

M. Valentino received her MS degree in electronic engineering in 1992. She received the degree of specialist in telecommunication in 1993. She has worked as a researcher for ALENIA since 1994.